

Experimental research on structure-borne noise at pulse-width-modulation excitation

Janez Luznar^a, Janko Slavič^b, and Miha Boltežar^b

^a*Domel, d.o.o., Otoki 21, 4228 Železniki, Slovenia*

^b*Faculty of Mechanical Engineering, University of Ljubljana, Aškerčeva 6, 1000 Ljubljana, Slovenia*

Cite as:

Janez Luznar, Janko Slavič, Miha Boltežar

Experimental research on structure-borne noise at pulse-width-modulation excitation

Applied Acoustics, Vol. 137, p. 33-39, 2018

DOI: 10.1016/j.apacoust.2018.03.005

Abstract

Pulse-width modulation (PWM) is widely used in motor control and represents a carrier-frequency-dependent structural excitation. The PWM's excitation harmonics are also reflected in an air gap's electromagnetic forces, the transmitted bearing forces and the resulting structure-borne noise. Inappropriate carrier-frequency selection can cause additional electromagnetic noise. The latter can be reduced by a characterization of the coupling between the excitation harmonics and the structural dynamics. To obtain a clear insight into the physical phenomenon, an experiment with original motor parts is proposed, which introduces bearing force measurement and excludes the aerodynamic and mechanical sources of noise. The detailed dependence of the structure-borne noise on the PWM carrier frequency can be obtained by dense carrier-frequency measurements. The experimental results show that even at higher frequencies (above 10 kHz), the carrier-frequency selection can cause a 25 dB(A) difference in the total sound pressure level. The switching noise of PWM controlled machines can be reduced by the appropriate carrier-frequency selection in accordance with the structural dynamics.

Keywords: Bearing forces, experiment, PWM carrier frequency, structural dynamics, structure-borne noise.

1. Introduction

In permanent-magnet synchronous motors (PMSMs) the variable speed can be controlled by pulse-width modulation (PWM), which composes current waveforms of the desired fundamental frequency component together with a number of higher switching harmonics [1]. The latter enriches the Maxwell force spectrum [2]. The general PWM principles are based on a constant carrier frequency, which result in a concentrate unpleasant noise spectrum [3], but still many times indicate lower overall noise than random modulation techniques [4], [5]. The latter represent wide frequency domain excitation [6], interacting with many modal modes, where one or two can be simultaneously eliminated, as shown by Chai *et al.* [7]. However, to avoid any mode excitation, the proposed research focused on constant carrier techniques and selecting an appropriate carrier frequency.

PMSMs contain different sources of acoustic noise: mechanical, aerodynamic and electromagnetic [8]. To anticipate and investigate the electromagnetic noise, analytical models have been developed, which indicate good agreements between computation and experiment by applying the forces on stator only [9]. Further, the strong impact of the supply harmonics on the noise of synchronous machines was shown by coupling the 2D electromagnetic and 3D structural finite element (FE) models [2]. Torregrossa *et al.* [10] proposed a 3D FE model to evaluate the electromagnetic vibration up to 5 kHz, but the frequency range of the numerical prediction is

limited by the structural model's validation with experimental modal analysis [11]. Since the modal parameters only match up to a few kHz [12]–[16], the electromagnetic noise predictions at higher frequencies have limited credibility.

There are also experimental investigations of the acoustic noise for PWM-controlled motors that show a dependence on different motor types, motor powers, rotor speeds, PWM techniques and the carrier frequency [17]. Binojkumar *et al.* [3] studied the acoustic noise at different fundamental frequencies and over a range of carrier frequencies, but we believe a denser carrier-frequency arrangement is necessary to obtain a detailed PWM excitation coupling with structural dynamics. Blaabjerg *et al.* [18] proposed the random PWM excitation and acoustic measurement to identify the transfer function of mechanical structure. The latter was used by Mathe *et al.* [19] to approximate the force spectrum, based on the input voltage spectrum. However, there is still a lack of experimental investigation, focusing on PWM switching noise reduction at dense PWM carrier frequency excitations.

The electromagnetic forces have been identified as the main cause of noise and vibration in PMSM [9]. There are methods to measure the unbalanced magnetic forces [20]–[22] and to characterize the force excitation harmonics, e.g., directly by dynamic force measurements [23] or indirectly by FEM transfer functions and measured vibration data [24]. Nevertheless, there is still a lack of experimentally identified PWM excitation forces, coupled with structural dynamics.

The aim of our investigation was to experimentally research the influence of the PWM carrier-frequency on the bearing forces and structure-borne noise. An experimental approach is

introduced, where the system's complexity is minimized by using only one excitation coil, half of the stator stack and a fixed rotor. The preliminary researched structural dynamics enables a better understanding of the coupling between the PWM excitation harmonics and the response of the bearing forces. Densely spaced carrier-frequency measurements show a strong variation in the structure-borne noise and indicate that the appropriate carrier-frequency selection is important even at higher frequencies (above 10 kHz).

The manuscript is organized as follows. Section 2 shows the PWM excitation, Section 3 shows the structural dynamics, Section 4 shows the experimental setup, Section 5 shows the results and discussion, Section 6 draws the conclusions and Section 7 presents the perspectives.

2. PWM excitation

The acoustic noise in electric motors has many sources due to diverse electromagnetic, mechanical and aerodynamic phenomena [8]. The main source of acoustic noise for low- and medium-speed motors has an electromagnetic origin [17], which is especially broadband in the case of inverter-fed electric motors [25]. The process of structure-borne noise generation at PWM excitation is shown in Fig. 1. The PWM excitation harmonics cause electromagnetic forces, which interact with the structural dynamics. Every frequency component of the force has its own effect upon the structure and therefore contributes to the surface vibration, causing the electromagnetically induced noise.

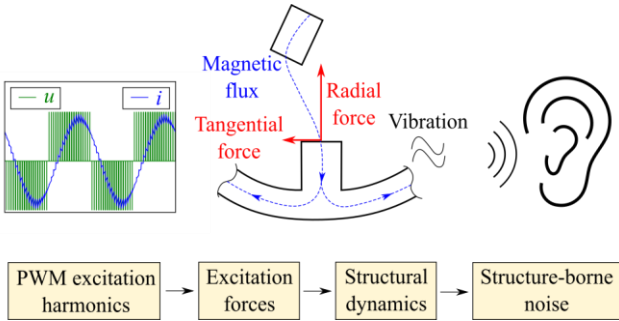


Fig. 1: Structure-borne noise at PWM excitation.

2.1. PWM excitation harmonics

In applications a sine-triangle PWM is very common [3], where the sinusoidal modulating signal at frequency f_1 and amplitude U_1 is compared with the triangular carrier signal at frequency f_c and amplitude U_c . In the linear modulating region ($m_a \leq 1$), the amplitude of the fundamental component varies linearly with the modulation index m_a [26]

$$m_a = U_1/U_c \quad (1)$$

and the frequency contents involve the fundamental component f_1 with additional switching harmonics at the frequencies f_h [10]:

$$f_h = n \cdot f_c \pm k \cdot f_1 \quad (2)$$

where $n = 1, 2, 3, \dots$, and f_c is the carrier frequency. When n is even, $k = \pm 2, \pm 4, \dots$ and when n is odd, $k = \pm 1, \pm 5, \dots$. The voltage harmonics for sine-triangle PWM excitation with the parameters $f_1 = 100$ Hz, $m_a = 0.8$ and $f_c = 4000$ Hz are shown in Fig. 2.

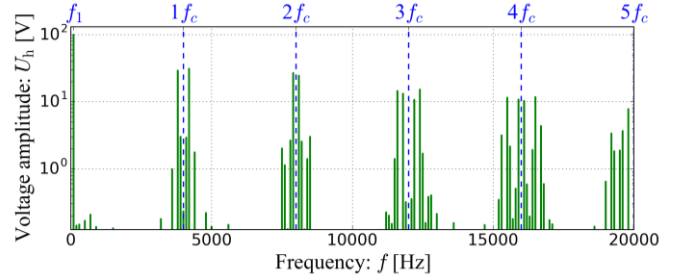


Fig. 2: Frequency contents of the voltage excitation harmonics for a sine-triangle PWM

The PWM voltage excitation harmonics depend on the carrier type, the carrier frequency f_c , the fundamental frequency f_1 and the modulation index m_a [26]. By increasing the carrier frequency f_c , the frequencies of the switching harmonics f_h increase, whereas by increasing the fundamental frequency f_1 , the frequencies of the switching harmonics f_h become more dispersed [27].

Variable speed control is achieved by adjusting the fundamental frequency f_1 and the modulation index m_a . The latter does not affect the frequencies of the PWM excitation harmonics, but varies their amplitudes. Fig. 3 shows the evolution of the sine-triangle PWM voltage harmonics' amplitudes as a function of the modulation index m_a . It is evident that a variable motor load results in different proportions of the switching harmonics in the PWM voltage excitation and therefore the structure-borne noise minimization is a complex task.

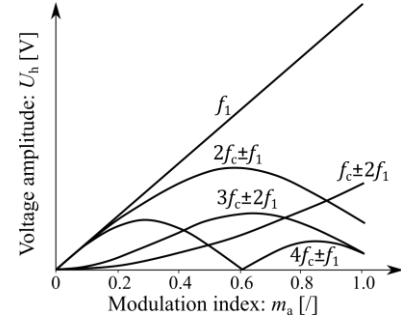


Fig. 3: Evolution of the sine-triangle PWM voltage harmonic amplitudes as a function of the modulation index m_a [28]

2.2. Excitation forces

The PWM voltage harmonics excite the stator coils, which form the magnetic field; consequently, the excitation harmonics also occur in the air-gap magnetic flux B [29] and the air-gap Maxwell pressure distribution σ [30]:

$$\sigma_r = \frac{1}{2\mu_0} (B_r^2 - B_c^2) \quad (3)$$

$$\sigma_t = \frac{1}{\mu_0} B_r B_t \quad (4)$$

where μ_0 is the permeability of free space, r is the radial and t is the tangential direction. The Maxwell pressure distribution over the rotor-stator air-gap surface (S) can be transformed to the Cartesian coordinate system (σ_x, σ_y), resulting in the electromagnetic force components F_x and F_y [21]:

$$F_x = \int_S \sigma_x dS, \quad (5)$$

$$F_y = \int_S \sigma_y dS \quad (6)$$

which are transmitted to the bearing location and can be measured as proposed in this investigation. Higher carrier frequencies result in lower magnetic flux harmonics [29] and consequently in lower electromagnetic force harmonics. Nevertheless, as shown later in Section 5.1, the selection of higher PWM carrier-frequency can also cause more distorted bearing forces, due to the interaction with structural dynamics.

3. Structural dynamics

3.1. General impact on the structure-borne noise

Structure-borne noise results from the excitation of the modal modes. These are the inherent properties of a structure and represent different deflection shapes, which can be excited with electromagnetic forces inside the electrical machine [17]. Force excitations make the laminated core oscillate, and these oscillations are also transmitted to other components, such as the shaft, bearing, yoke and housing. If the frequencies of the exciting forces are near to the system's natural frequencies, the noise significantly increases [8]. The PWM switching harmonics' interaction with the structural dynamics cause high-frequency, structure-borne noise, which is irritating if the frequencies are within the human audible frequency range (20 Hz to 20 kHz) [3]. PWM harmonics are unavoidable, but structure-borne noise can be minimized by the appropriate carrier-frequency selection in accordance with the structural dynamic properties of the system.

The frequency-response function (FRF) is a fundamental measurement that isolates the inherent dynamic properties of a mechanical structure. The FRF describes the input-output relationship between two points on a structure as a function of the frequency [31]. This investigation uses the force transmission FRF as a measure of how much force response a structure has at the bearing location (F_b) per unit of electromagnetic force excitation in an air gap (F_e):

$$H(f) = \frac{F_b(f)}{F_e(f)} \quad (7)$$

To avoid the resonance phenomenon, the excitation force harmonics should exclude the amplified regions in the FRF. If the resonance cannot be avoided, there is also the possibility to

modify the FRF, e.g., by using a damping layout, determined via the spatial damping identification methods [32].

3.2. Structural dynamics of excitation and measurement unit

Excitation and measurement unit is detailed later in Section 4.1, but this section provides preliminary researched structural dynamics with the force-transmission FRF (7). The identification process and the coordinate systems are characterized in Fig. 4. The impact force hammer was used for the system excitation at the rotor's center and the response was measured with force sensors at the bearing location. The investigated frequency range depends on the frequency-excitation capabilities of the impact tip. The applied steel impact tip was able to excite well the frequency range up to 4000 Hz.

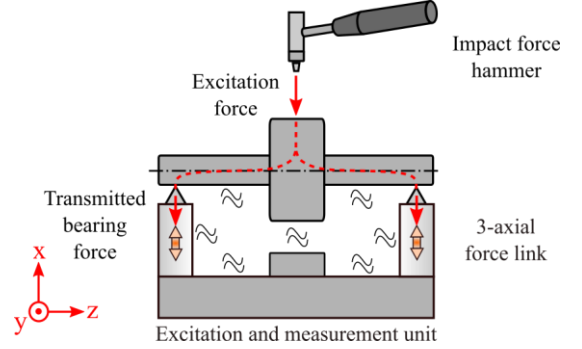


Fig. 4: Identification of the force-transmission frequency-response function

Fig. 5 shows the magnitude of the measured force transmission FRF in the y direction and characterizes two different carrier frequencies in the FRF region, used later in Section 5.1. The FRF represents the frequency-dependent transfer function from the rotor center (position of electromagnetic force excitation) to the bearing location (position of dynamic force sensors). Therefore, the force transmission FRF also represents a coupling between the electromagnetic excitation forces and the transmitted bearing forces. The FRF is a consequence of the structural dynamics and is magnified around the natural frequencies of the system (628 Hz, 1615 Hz, 2063 Hz and 3881 Hz).

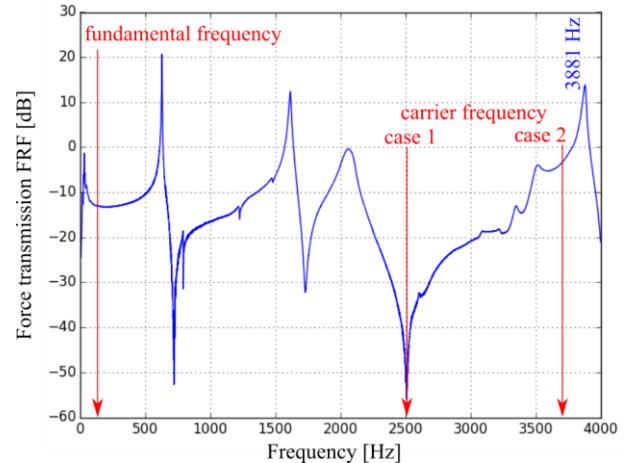


Fig. 5: Force-transmission FRF for the excitation and measurement unit

4. Experiment: PWM excited structural dynamics

4.1. Excitation and measurement unit

Structure-borne noise results from the interaction between the PWM switching harmonics and the structural dynamics. To investigate their coupling an excitation and measurement unit is proposed, shown in Fig. 6. This unit contains the stator, rotor (fixed), air gap, shaft, force links, aluminium frame and PWM excitation. The rotor and stator are taken from an 8-pole, 12-slot PMSM motor with a stack length of 22 mm and an air gap length of 0.4 mm. An aluminum frame is used to avoid changes in the magnetic paths. The stator core is held rigid during the test, whereas the rotor bearings are replaced with a 3-axial force link Kistler 9317B. The force sensors measure the dynamic forces in three directions (x, y, z).

The system complexity is minimized by using only one excitation coil and half of the stator stack. Similarly as Mathe *et al.* [19], the research isolated PWM noise by excluding the rotor's rotation and consequently eliminating all the sources of mechanical noise (imbalance, bearings, sliding contacts, gears) and aerodynamic noise (cooling fans, rotor windage).

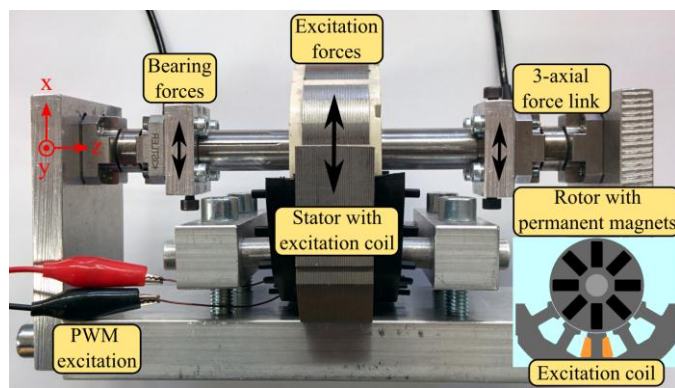


Fig. 6: Excitation and measurement unit – front and right view

4.2. Experimental set-up

The experimental set-up for a structure-borne noise investigation at PWM excitation is shown in Fig. 7. It contains the following elements: computer, digital output module, single-phase full-bridge inverter, anechoic chamber, excitation and measurement unit, transducers and analog input modules.

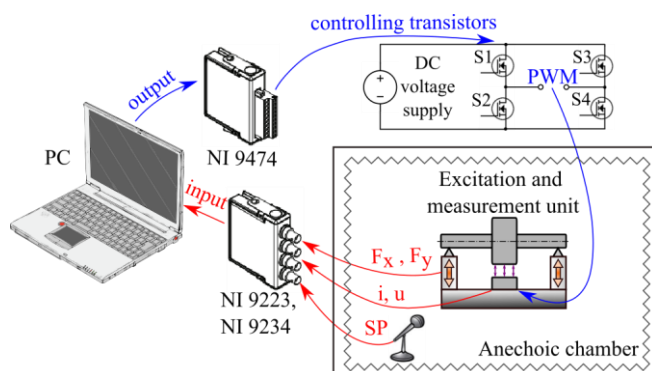


Fig. 7: Experimental set-up for structure-borne noise at PWM excitation

The computer controls the process of generating the custom PWM excitation and acquiring the measurement signals. The process involves three subgroups:

4.2.1. Custom PWM excitation

The program code to generate the PWM excitations for different PWM parameters: carrier type, carrier frequency, fundamental frequency and amplitude was developed from scratch. The code generates a Boolean array, which is sent to the digital output module NI 9474. The latter controls the transistors in a single-phase, full-bridge inverter [26], which generates a sequence of pulses with the height of the DC voltage supply. The generated PWM excitation contains different voltage harmonics, depending on the chosen PWM parameters; in the case of the sine-triangle PWM technique the frequencies of the switching harmonics are defined by (2).

4.2.2. PWM excitation of the excitation and measurement unit

The custom PWM voltage excitation generated on a single-phase, full-bridge inverter is sent further to the stator excitation coil on the excitation and measurement unit. The stator coil excitation produces a magnetic field, where the PWM voltage harmonics transform to the air-gap magnetic flux density harmonics. As shown in equations (3), (4), the magnetic field harmonics also reflect in the air-gap Maxwell pressure distribution. Furthermore, the cumulative effect of the pressure distribution on the surface forms electromagnetic forces (5), (6), which transmit through the dynamic structure and result in bearing forces and also in structure-borne noise. The bearing forces and structure-borne noise both represent a response quantities, sharing the same structural dynamics.

4.2.3. Acquired measurement signals

On the computer's input side, the analog input modules NI 9223 and NI 9234 are used for the data acquisition. Table 1 shows the measured signals, the associated transducers and their measuring points.

Table 1

Measured signals, associated transducers and measuring points

| Measured signal | Transducer | Measuring point |
|-----------------|-----------------|---------------------|
| Voltage | Voltage divider | On excitation coil |
| Current | Shunt resistor | On excitation coil |
| Force | Kistler 9317B | At rotor bearings |
| Sound pressure | PCB 130E21 | In anechoic chamber |

A voltage measurement verifies the properly generated PWM excitation, the current measurement estimates the magnetic field, the force measurement represents the bearing forces due to the interaction of PWM excitation with structural dynamics, and the sound pressure measurement in the anechoic chamber is used to evaluate the structure-borne noise at the PWM excitation. The microphone is placed 1 m in x direction above the excitation and measurement unit. The voltage, current and forces were measured at a sampling rate of 1 MHz and the sound pressure at 51.2 kHz. The latter meets the Nyquist frequency limit, since the interested frequency range for the acoustic noise observation is limited to 20 kHz.

5. Results and discussion

5.1. Bearing forces at PWM excitation

The excitation and measurement unit enables measurements of the bearing forces at PWM excitation when coupled with the structural dynamics. The proposed bearing forces globally differ from that in complete electric motor [9], but locally represent comparable forces on individual stator tooth. Different PWM coil excitations were performed and compared with the current and bearing force measurements. The results include sine-triangle PWM with equal fundamental components f_1 at 100 Hz, but two different carrier frequencies f_c : 2.5 kHz (case 1) and 3.7 kHz (case 2), as shown in Fig. 5. The time and frequency domains of the *current* and *bearing force* are shown in Fig. 8 (case 1) and Fig. 9 (case 2), while the RMS numerical comparison is shown in Table 2.

The excitation with a higher carrier frequency features a *less distorted current waveform*, but in contrast, the transmitted *bearing force is significantly more distorted*. The total RMS of the excitation currents are the same for both cases (0.73 A), but the total RMS of the bearing force is more than 30% higher for case 2. The additional distortion is mainly due to the PWM switching harmonic and its interaction with the natural frequency of the system (3881 Hz, Fig. 5). The maximal force PWM switching-harmonic RMS value is *more than 65 times higher for case 2*, although the associated current harmonic is lower (0.04 A instead of 0.06 A). Inappropriate carrier-frequency selection can result in a significantly higher force switching harmonics, which could lead to the unpleasant tonal noise to the human ear.

Table 2

RMS values for different excitation cases

| Case [1] | f_c [kHz] | Total | | Maximal PWM switching harmonic | | |
|-------------|----------------|------------------|------------------|-----------------------------------|------------------|------------------|
| | | I_{RMS} [A] | F_{RMS} [N] | f_i [kHz] | I_{RMS} [A] | F_{RMS} [N] |
| 1 | 2.5 | 0.73 | 10.35 | 2.7 | 0.06 | 0.14 |
| 2 | 3.7 | 0.73 | 13.96 | 3.9 | 0.04 | 9.18 |

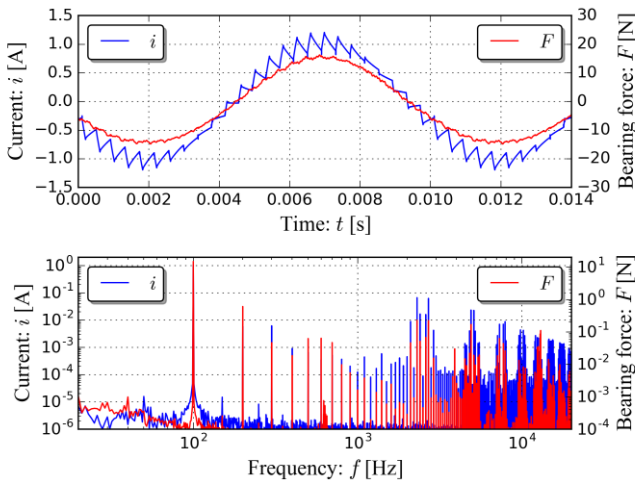


Fig. 8: PWM excitation with carrier frequency at 2.5 kHz and resulting bearing force in the time and frequency domains

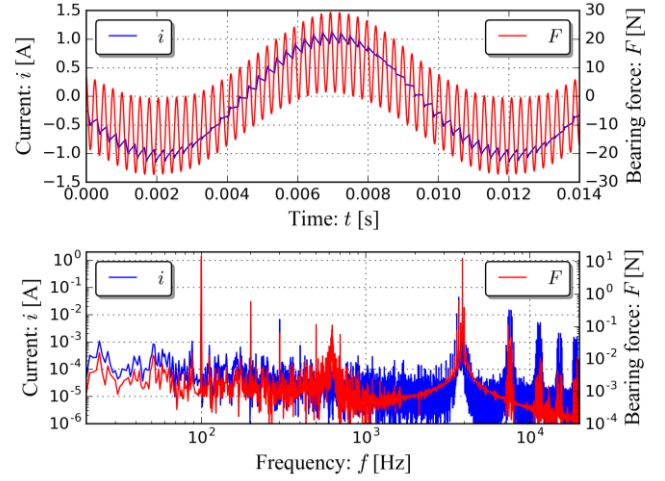


Fig. 9: PWM excitation with carrier frequency at 3.7 kHz and resulting bearing force in the time and frequency domains

5.2. Structure-borne noise at PWM excitation

The excitation and measurement unit enables a clear experimental identification of the structure-borne noise at PWM excitation. Previous investigations [3], [17], [27], [33] tested the noise's dependence on the carrier frequency only at a few different carrier frequencies. To obtain a full insight into the coupling between the PWM excitation and the structural dynamics, a dense carrier-frequency arrangement is necessary. In this way Fig. 10 is post-processed from 331 different measurements for sine-triangle PWM excitations with the same fundamental component f_1 (60 Hz), but different carrier frequencies f_c (240, 300, 360, ... 20040 Hz). The graph involves the sound-pressure-level total curve and frequency contents, both as a function of the PWM carrier frequency. The intensity graph represents the sound-pressure-level frequency contents, where louder regions occur whenever one of the PWM switching harmonics coincides with any natural frequency horizontal line. The PWM excitation harmonics, causing the resonant phenomenon, also increase the total sound-pressure-level (magenta curve in Fig. 10).

The preliminary investigated frequency-response function in Fig. 5 and the total sound-pressure-level curve in Fig. 10 show peaks at the same frequencies. Therefore the coupling of the structural dynamics is also expressed in the total sound-pressure-level curve. Increasing the PWM carrier frequency decays the total sound-pressure-level overall, but interaction of the PWM switching harmonics with system's natural frequencies raises the noise within the entire tested PWM carrier-frequency range. A *strong dependence is shown even at higher carrier frequencies (above 10 kHz)*, where the numerical predictions have limited credibility. By changing the carrier frequency from 14 kHz to 11 kHz, the total sound-pressure-level of the electromagnetic noise can be reduced for more than 25 dB(A) on the excitation and measurement unit.

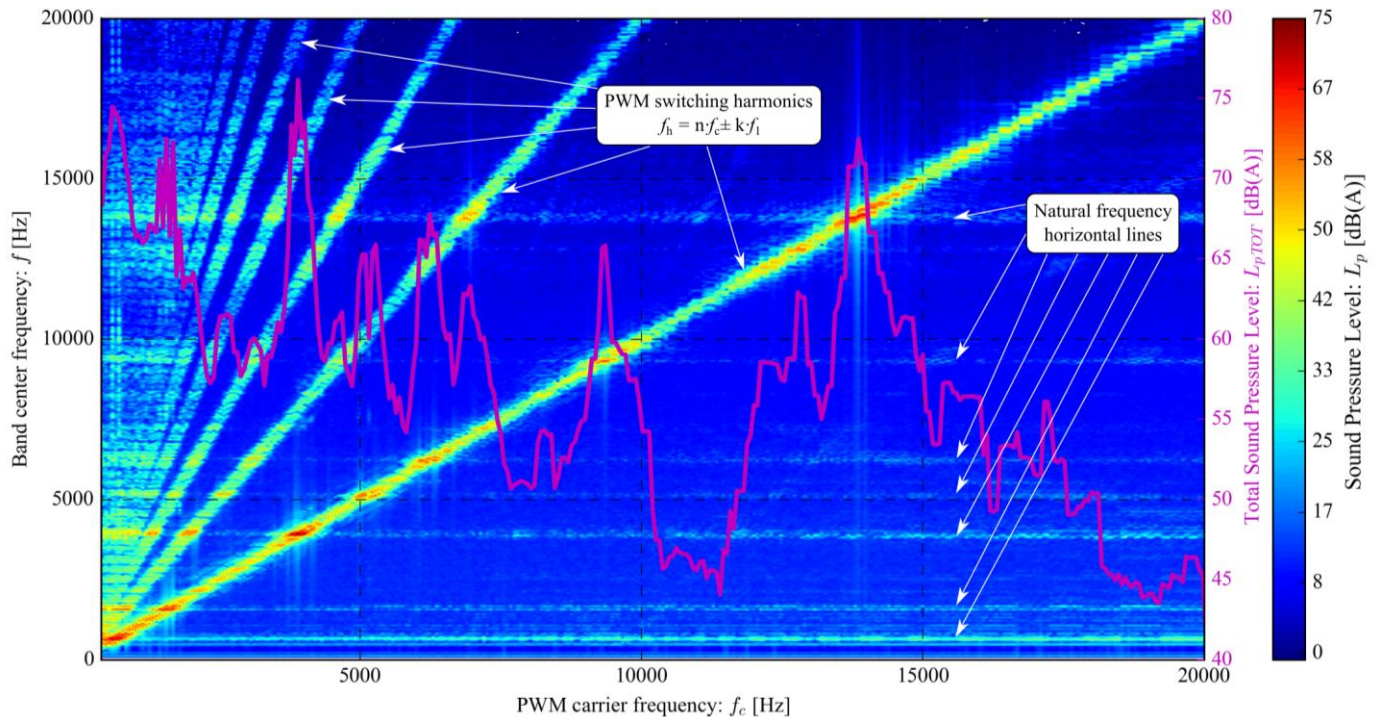


Fig. 10: Sound-pressure-level frequency contents and total level for 331 different PWM excitations involving the same fundamental component, but different carrier frequencies

5.3. Structure-borne noise variation due to PWM parameters

Variable speed control requires a variation of the fundamental frequency (f_1) and its amplitude (m_a). To investigate their impact on the structure-borne noise, the procedure from Section 5.2 was repeated for different PWM parameters. The excitation and measurement sequences were automated with a custom code and it took about 10 minutes to obtain all 331 measurements for one curve dependency.

Fig. 11 characterizes the total sound-pressure-level dependence on the carrier-frequency for the PWM excitations with different fundamental frequencies (f_1). Increasing the fundamental frequency f_1 spreads the PWM switching harmonics (2) and thus reduces the probability for multiple excitations of the same system's natural frequency; consequently, the peaks in the total sound-pressure-level curve are reduced. Additionally, the low-noise frequency regions remain at the same carrier frequencies.

Furthermore, Fig. 12 shows that a significantly stronger influence on the total sound-pressure-level comes from the variation of the modulation index (m_a), which can result in a difference of up to 20 dB(A). The latter results from a different proportion of the switching harmonics in the PWM voltage excitation (Fig. 3) and is unavoidable in the case of a variable motor load. However, a favorable finding is that the low PWM switching noise regions still remain within the same PWM carrier-frequency range.

To reduce the switching noise of PWM-controlled machines the anti-resonant carrier-frequency regions (e. g., around 11 kHz for proposed experiment) can be identified by a densely spaced carrier-frequency measurements.

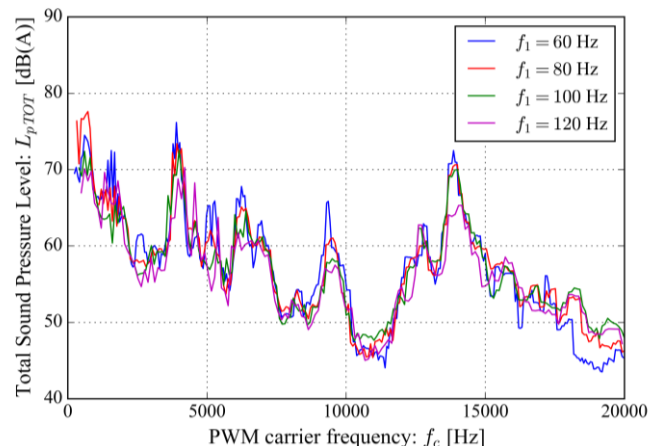


Fig. 11: Total sound-pressure-level dependence from the carrier frequency for different fundamental frequencies (f_1)

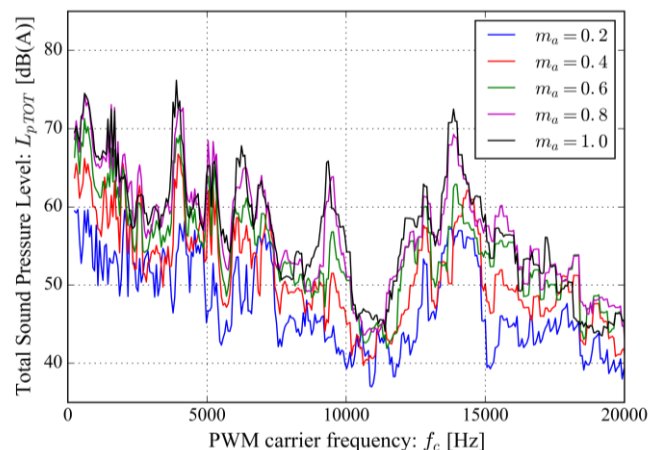


Fig. 12: Total sound-pressure-level dependence from the carrier frequency for different modulation indexes (m_a)

6. Conclusions

The proposed research represents clear insight into the PWM excited structural dynamics. An excitation and measurement unit is proposed, containing all main motor parts, but excluding the rotor's rotation to isolate the PWM effects from other excitation sources. The transmitted bearing forces and the structure-borne noise are experimentally investigated at different PWM excitations. Both investigated quantities share the same structural dynamics and therefore indicate similar frequency dependent coupling.

To reduce the electromagnetic structural excitation and consequently the noise, the transmitted bearing force should be minimized. Its elimination is not possible, because of the fundamental component, but the appropriate selection of the PWM carrier frequency can *reduce the PWM distortion harmonics* to a negligible level. The transmitted bearing force depends on the electromagnetic force excitation and also on the structural properties. The excitation frequency contents close to the system's natural frequencies are amplified in accordance with the force-transmission frequency-response function. The appropriate carrier-frequency selection should consider the regions with a low force-transmission factor.

The coupling between the PWM excitation and the structural dynamics also influences the structure-borne noise. An experimental investigation with a dense carrier-frequencies distribution shows that even at higher carrier frequencies (e.g., above 10 kHz) the coupling effect can cause a 25 dB(A) difference in the total sound-pressure-level. Furthermore, by comparing the measurements for different PWM parameters: fundamental amplitudes and modulation indexes (i.e., variable motor speed and load), a favorable finding is that low structure-borne noise regions still remain in the same PWM carrier-frequency range.

7. Perspectives

The proposed test bench could be used also to study the magnetic unbalanced effects on bearings, to study the effects of bearing forces on the machine lifetime, to identify the interface forces in the field of dynamic substructuring [34] or to study the bearings as a complex joint, which is better handled separately via substructuring [35].

To ensure a low structure-borne PWM switching noise, the appropriate carrier-frequency can be identified with a dense carrier-frequency measurement distribution to find the low-noise (i.e., anti-resonant) frequency regions. By using the automated excitation and measurement sequences, the low-noise regions for any PWM-controlled machine can be obtained in a few minutes.

References

- [1] J. T. Boys and P. G. Handley, "Harmonic analysis of space vector modulated PWM waveforms," *IEE Proc. B Electr. Power Appl.*, vol. 137, no. 4, pp. 197–204, 1990.
- [2] P. Pellerey, V. Lanfranchi, and G. Friedrich, "Coupled Numerical Simulation Between Electromagnetic and Structural Models. Influence of the Supply Harmonics for Synchronous Machine Vibrations," *IEEE Trans. Magn.*, vol. 48, no. 2, pp. 983–986, 2012.
- [3] A. C. Binojkumar, B. Saritha, and G. Narayanan, "Acoustic Noise Characterization of Space-Vector Modulated Induction Motor Drives — An Experimental Approach," *IEEE Trans. Ind. Electron.*, vol. 62, no. 6, pp. 3362–3371, 2015.
- [4] L. Mathe, F. Lungeanu, P. O. Rasmussen, and J. K. Pedersen, "Asymmetric Carrier Random PWM," *2010 IEEE Int. Symp. Ind. Electron.*, pp. 1218–1223, 2010.
- [5] L. Mathe, "Product sound: Acoustically pleasant motor drives," 2010.
- [6] J. T. Boys and P. G. Handley, "Spread spectrum switching: low noise modulation technique for PWM inverter drives," *IEE Proc. B Electr. Power Appl.*, vol. 139, no. 3, pp. 252–260, 1992.
- [7] J. Y. Chai, Y. H. Ho, Y. C. Chang, and C. M. Liaw, "On acoustic-noise-reduction control using random switching technique for switch-mode rectifiers in PMSM drive," *IEEE Trans. Ind. Electron.*, vol. 55, no. 3, pp. 1295–1309, 2008.
- [8] S. Lakshmikanth, K. R. Natraj, and K. R. Rekha, "Noise and Vibration reduction in Permanent Magnet Synchronous Motors - A Review," *Int. J. Electr. Comput. Eng.*, vol. 2, no. 3, pp. 405–416, 2012.
- [9] R. Islam and I. Husain, "Analytical model for predicting noise and vibration in permanent-magnet synchronous motors," *Ind. Appl. IEEE Trans.*, vol. 46, no. 6, pp. 2346–2354, 2010.
- [10] D. Torregrossa, D. Paire, F. Peyraut, B. Fahimi, and A. Miraoui, "Active mitigation of electromagnetic vibration radiated by PMSM in fractional-horsepower drives by optimal choice of the carrier frequency," *IEEE Trans. Ind. Electron.*, vol. 59, no. 3, pp. 1346–1354, 2012.
- [11] M. Javorski, G. Čepon, J. Slavič, and M. Boltežar, "A generalized magnetostrictive-forces approach to the computation of the magnetostriction-induced vibration of laminated steel structures," *IEEE Trans. Magn.*, vol. 49, no. 11, pp. 5446–5453, 2013.
- [12] M. Pirnat, G. Čepon, and M. Boltežar, "Introduction of the linear contact model in the dynamic model of laminated structure dynamics: An experimental and numerical identification," *Mech. Mach. Theory*, vol. 64, pp. 144–154, 2013.
- [13] M. Mair, B. Weilharter, S. Rainer, K. Ellermann, and O. Biró, "Numerical and experimental investigation of the structural characteristics of stator core stacks," *COMPEL Int. J. Comput. Math. Electr. Electron. Eng.*, vol. 32, no. 5, pp. 1643–1664, 2013.
- [14] P. Millithaler, É. Sadoulet-Reboul, M. Ouisse, J.-B. Dupont, and N. Bouhaddi, "Structural dynamics of electric machine stators : Modelling guidelines and identification of three-dimensional equivalent material properties for multi-layered orthotropic laminates," *J. Sound Vib.*, vol. 348, pp. 185–205, 2015.
- [15] P. Millithaler, E. Sadoulet-Reboul, M. Ouisse, J.-B. Dupont, and N. Bouhaddi, "Identification of representative anisotropic material properties accounting for friction and preloading effects: A contribution for the modeling of structural dynamics of electric motor stators," *J. Vib. Control*, pp. 1–23, 2016.
- [16] F. Lin, S. Zuo, W. Deng, and S. Wu, "Modeling and Analysis of Electromagnetic Force, Vibration, and Noise in Permanent-Magnet Synchronous Motor Considering Current Harmonics," *IEEE Trans. Ind. Electron.*, vol. 63, no. 12, pp. 7455–7466, 2016.
- [17] S. L. Capitaneanu, B. de Fernel, M. Fadel, and F. Jadot, "On the Acoustic Noise Radiated by PWM AC Motor Drives," *Autom. J. Control. Meas. Electron. Comput. Commun.*, vol. 44, no. 3–4, pp. 137–145, 2003.
- [18] F. Blaabjerg, J. K. Pedersen, E. Ritchie, P. Nielsen, and S. Member, "Determination of mechanical resonances in induction motors by random modulation and acoustic measure - Industry Applications, IEEE Transactions on," vol. 31, no. 4, pp. 823–829, 1995.
- [19] L. Mathe, U. Jakobsen, P. O. Rasmussen, and J. K. Pedersen, "Analysis of the Vibration Spectrum Based on the Input Voltage Spectrum," no. 2, pp. 220–225, 2009.
- [20] T. J. E. Miller, "Faults and unbalance forces in the switched reluctance machine," *IEEE Trans. Ind. Appl.*, vol. 31, no. 2, pp. 319–328, 1995.
- [21] Z. Q. Zhu, D. Ishak, D. Howe, and J. Chen, "Unbalanced magnetic forces in permanent-magnet brushless machines with diametrically asymmetric phase windings," *IEEE Trans. Ind. Appl.*, vol. 43, no. 6, pp. 1544–1553, 2007.
- [22] C. I. Lee and G. H. Jang, "Experimental Measurement and Simulated Verification of the Unbalanced Magnetic Force in Brushless DC Motors," *IEEE Trans. Magn.*, vol. 44, no. 11, 2008.

- [23] A. Brković, J. Slavič, and M. Boltežar, "Typical bearing-fault rating using force measurements: application to real data," *J. Vib. Control*, vol. 17, no. 14, pp. 2164–2174, 2011.
- [24] "The Force Identification of 200kW IPMSM Using Phase Reference Spectrum," in *IEEE Transportation Electrification Conference and Expo, Asia-Pacific*, 2016, pp. 818–821.
- [25] J. Le Besnerais, V. Lanfranchi, M. Hecquet, and P. Brochet, "Characterization and Reduction of Audible Magnetic Noise Due to PWM Supply in Induction Machines," *IEEE Trans. Ind. Electron.*, vol. 57, no. 4, pp. 1288–1295, 2010.
- [26] M. H. Rashid, *Power Electronics Handbook*, Third Edit. Elsevier, 2011.
- [27] I. P. Tsoumas and H. Tischmacher, "Influence of the Inverter's Modulation Technique on the Audible Noise of Electric Motors," *IEEE Trans. Ind. Appl.*, vol. 50, no. 1, pp. 269–278, 2012.
- [28] S. Ueda, K. Honda, T. Ikimi, M. Hombu, and S. Member, "Magnetic Noise Reduction Technique for an AC Motor Driven by a PWM Inverter," *IEEE Trans. Power Electron.*, vol. 6, no. 1, 1991.
- [29] H. Kaihara, N. Takahashi, M. Nakano, M. Kawabe, T. Nomiyama, A. Shiozaki, and D. Miyagi, "Effect of Carrier Frequency and Circuit Resistance on Iron Loss of Non-Oriented Electrical Steel Sheet under Single-Phase Full-Bridge PWM Inverter Excitation," *Electr. Eng. Japan*, vol. 192, no. 2, pp. 49–57, 2015.
- [30] F. Druesne, J. Hallal, P. Lardeur, and V. Lanfranchi, "Modal stability procedure applied to variability in vibration from electromagnetic origin for an electric motor," *Finite Elem. Anal. Des.*, vol. 122, pp. 61–74, 2016.
- [31] B. J. Schwarz and M. H. Richardson, "Experimental Modal Analysis," in *CSI Reliability Week*, 1999, pp. 1–12.
- [32] M. Brumat, J. Slavič, and M. Boltežar, "Design of damping layout using spatial-damping identification methods," *Int. J. Mech. Sci.*, pp. 1–13, 2016.
- [33] W. C. Lo, C. C. Chan, Z. Q. Zhu, L. Xu, D. Howe, and K. T. Chau, "Acoustic Noise Radiated by PWM-Controlled Induction Machine Drives," *IEEE Trans. Ind. Electron.*, vol. 47, no. 4, pp. 880–889, 2000.
- [34] T. Kranjc, J. Slavič, and M. Boltežar, "An interface force measurements-based substructure identification and an analysis of the uncertainty propagation," *Mech. Syst. Signal Process.*, vol. 56–57, pp. 2–14, 2014.
- [35] M. Razpotnik, T. Bischof, and M. Boltežar, "The influence of bearing stiffness on the vibration properties of statically overdetermined gearboxes," *J. Sound Vib.*, vol. 351, pp. 221–235, 2015.